Current Applied Physics 13 (2013) 53–59

Contents lists available at SciVerse ScienceDirect

Current Applied Physics

journal homepage: www.elsevier.com/locate/cap

Two diodes model and illumination effect on the forward and reverse bias $I-V$ and $C-V$ characteristics of Au/PVA (Bi-doped)/n-Si photodiode at room temperature

S. Demirezen [a,*], Ş. Altındal [a], İ. Uslu [b]

[a] Physics Department, Faculty of Sciences, Gazi University, Besevler, Ankara, Turkey
[b] Chemistry Education Department, Faculty of Education, Gazi University, Ankara, Turkey

ARTICLE INFO

Article history:
Received 14 March 2012
Received in revised form
6 May 2012
Accepted 12 June 2012
Available online 21 June 2012

Keywords:
Photodiode
Illumination effect
Interface states
Series and shunt resistance

ABSTRACT

The forward and reverse bias current–voltage ($I-V$), capacitance/conductance–voltage ($C/G-V$) characteristics of the fabricated Au/PVA (Bi-doped)/n-Si photodiode have been investigated both in dark and under 250 W illumination intensity at room temperature. The energy density distribution profile of N_{ss} was extracted from the forward bias $I-V$ measurements by taking the voltage dependence of effective barrier height (Φ_e) and R_s for photodiode both in dark and under 250 W illumination cases. The exponential growth of the N_{ss} from midgap toward the bottom of the conductance band is very apparent for two cases. The obtained high value of n and R_s were attributed to the particular distribution of N_{ss} at metal/PVA interface, surface and fabrication processes, barrier inhomogeneity of interfacial polymer layer and the form of barrier height at M/S interface. While the values of C and G/w increase R_s and R_{sh} decrease under illumination, due to the illumination induced electron–hole pairs in depletion region. The voltage dependent N_{ss} profile was also obtained from the dark and illumination capacitance at 1 MHz and these values of N_{ss} are in good agreement. In addition, the fill factor (FF) under 250 W illumination level was found as 28.5% and this value of FF may be accepted sufficiently high. Thus, the fabricated Au/PVA (Bi-doped)/n-Si structures are more sensitive to light, proposing them as a good candidate as a photodiode or capacitance sensor for optoelectronic applications in modern electronic industry.

1. Introduction

When there is a thin interfacial insulator or polymer layer at metal/semiconductor (M/S) interface, MS type Schottky barrier diodes (SBDs) convert into metal–insulator/polymer–semiconductor (MIS) or (MPS) type SBDs or photodiode. The presence of such a thin interfacial layer may cause interface state charge with bias due to an additional electrical field in the interfacial layer and influences the diode electrical characteristics especially under illumination intensity [1–7].

Among them, Soylu and Yakuphanoğlu [1] have investigated the electrical and photovoltaic properties of the Au/n-GaAs SBD to possibility of use in photovoltaic applications as a solar cell. Uslu et al. [4], have investigated the illumination effect on main electrical parameters such as n, Φ_{B0}, W_D and N_D in Al–TiW–Pd_2Si/n-Si SBDs under dark and in the wide range of illumination levels at room temperature. They showed that the electrical characteristics of SBD are considerably affected under illumination. In addition, Yakuphanoğlu et al. [5] were also aimed to obtain the Au/organic dye/n-Si structure and determine the possibility of obtain solar cells with methylene blue interface. They showed that the performance of an SBD can be considerably the performance of device. Therefore, it can be said that, the interfacial parameters such as interface state density (N_{ss}), the thickness of the interfacial layer and the Schottky barrier inhomogeneity at M/S interface give rise to masking of the real electrical characteristics of SBD [5–10]. Among them, the most important one was carried out by Card and Rhoderick [9]. They fabricated the SBDs with interfacial films ranging from 8 to 26 Å in thickness, and their characteristics are related to this model. They showed that the effects of reduced transmission coefficients together with fixed charge in the film are investigated.

The series resistance (R_s) and shunt resistance (R_{sh}) of a diode are also important parameters, which cause the electrical characteristics of SBD to be non-ideal [11,12]. When a diode or solar cell has sufficient high R_s value (a few Ω), $I-V$ characteristics considerably deviate from the linearity especially at high forward bias

* Corresponding author. Tel.: +90 312 2021276; fax: +90 312 2122279.
E-mail address: s.demirezen@gazi.edu.tr (S. Demirezen).

1567-1739/$ – see front matter © 2012 Elsevier B.V. All rights reserved.
http://dx.doi.org/10.1016/j.cap.2012.06.009

region. On the other hand, when these devices have low R_{sh} value ($\leq$kΩ), leakage or reverse bias current becomes considerably high.

In recent years, polymer composite nanofibers have been used as interfacial layer between M/S interface instead of conventional insulating layer because of their large surface area to volume ratio and the unique nanometer scale architecture built by them [13–18]. In this respect, using an organic interfacial layer at M/S interface is cheaper than the conventional insulating layer and the fact that it can be synthesized with easier processes is promising due to low-cost, flexibility and lightness especially for photodiodes and solar cells. Among the polymer composite nanofibers, PVA nanofabrics have attracted much attention due to its unique chemical and physical properties as well as its industrial applications [17,19–22]. PVA has normally a poor electrical conductivity but this conductivity in PVA arises due to the high physical interactions between polymer chains, via hydrogen bonding between the hydroxyl groups [19] and the doping metals such as Ni, Zn [8], Bi [10] and Co [20] are mainly dominated by the properties of the amorphous regions [21]. Nanofiber which is a fiber with a diameter of nanometer order less than 1 μm (more typically 50–500 nm) provide a larger surface area per unit mass compared to that of films or the bulk material [14]. These polymer composite nanofiber films can be produced by using electro-spinning method. This method relies on electrostatic forces obtained by applying an electrical field by means of a DC high voltage source between the tip of a nozzle and a collector [18]. Electro-spinning occurs when the electrical forces at the surface of the drop overcome the surface tension of polymer solution. When this happens, the solution is ejected as an electrically charged jet and shoots toward the oppositely charged collector.

In this study, the forward and reverse bias I–V, C–V and G/w–V characteristics of the fabricated Au/PVA (Bi-doped)/n-Si photodiode have been investigated in dark and under 250 W illumination intensity at room temperature. The density distribution profile of N_{ss} was extracted from both the forward bias I–V measurements and the dark-illumination capacitance ($C_d - C_{ill}$) measurements at 1 MHz. Also, the influences of illumination on the main electrical parameters such as n, Φ_{Bo}, N_{ss}, R_{sh} and R_s of the photodiode have been investigated.

2. Experimental procedure

The fabrication of Au/PVA (Bi-doped)/n-Si photodiode, n-type (phosphor doped) single crystal silicon single crystal, with (111) surface orientation, 350 μm thickness and 0.7 Ω cm resistivity or doping concentration $N_D = 6.16 \times 10^{15}$ cm^{-3} was used. Si wafer was degreased in organic solution of peroxide–ammoniac solution in 10 min and then etched in a sequence of H_2O + HCl solution and then quenched in de-ionized water resistivity of 18 MΩ cm for a prolonged time. Preceding each cleaning step, the wafer was rinsed thoroughly in de-ionized water. Immediately after surface cleaning, high purity (99.999%) gold (Au) with a thickness of ~2000 Å was thermally evaporated onto the whole back side of Si wafer in a pressure about 10^{-6} Torr in high vacuum metal evaporation system. In order to perform a low resistivity ohmic back metal contact, n-Si wafer was sintered at about 450 °C for 5 min in N_2 atmosphere.

Immediately after the formation of ohmic contact, 0.5 g of bismuth acetate was mixed with 50 g of polyvinyl Alcohol (PVA), molecular weight = 72 000 and 9 ml of de-ionize water. After vigorous stirring for 2 h at 50 °C, a viscous solution of PVA/(Bi doped) acetates was obtained. The solution of the PVA (Bi-doped) was homogenized for 1.5 h by mixing with rotation before the deposition. The PVA (Bi-doped) nanofiber film on n-Si substrate was coated by electrospinning technique. Thus, the pure PVA was doped with Bi as 1% to increase their conductivity. Electrospinning process utilizes electrical force to produce polymer fibers. Electrospinning setup consists of four major components: The high-voltage power supply, the spinneret, the syringe pump and the electrically conductive collector. In this system, using a peristaltic syringe pump, the precursor solution was delivered to a metal needle syringe (10 ml) with an inner diameter of 0.9 mm at a constant flow rate of 0.02 ml/h. The needle was connected to a high voltage power supply and positioned vertically on a clamp. A piece of flat aluminum foil was placed 15 cm below the tip of the needle to collect the nanofibers. Si wafer was placed on the aluminum foil. Upon applying a high voltage of 20 kV on the needle, a fluid jet was ejected from the tip. The solvent evaporated and a charged fiber was deposited onto the Si wafer as a nonwoven mat. The thickness of interfacial layer PVA (d_i) was determined from the interfacial layer capacitance ($C_i = \varepsilon\varepsilon_o A/d_i$) as 79 Å, where, ε and ε_o are the permittivities of the semiconductor and interfacial layer, respectively. After spinning process, circular dots of 1 mm in diameter and 1000 Å thick high purity Au rectifying contacts were deposited on the PVA surface of the wafer through a metal shadow mask in high vacuum system in the pressure of about 10^{-7} Torr.

The forward and reverse bias I–V and admittance which are concluding C–V and G/ω–V measurements were performed by the use of a Keithley 2400 source meter and an HP 4192 An LF impedance analyzer and test signal of 40 mV_{rms} in dark and under illumination at room temperature, respectively. The measurements system was given in Fig. 1. All these measurements were carried out with the help of a microcomputer through an IEEE-488 AC/DC converter card. 250 W solar simulator (Model: 69931 Newport-Oriel Instruments, Stratford, CT, USA) was used as a light source. The photons at different power levels were passes through an AM1.5 filter which allowed wavelengths only between 400 and 700 nm to be incident upon the diodes.

3. Result and discussion

3.1. Effects of illumination on the I–V characteristics

For an MS Schottky diode and solar cell with a uniform thin interfacial insulator or organic material and R_s, the current through barrier according to the thermionic emission (TE) theory ($V \geq kT/q$) can be expressed as [9,11]:

$$I = I_o \exp\left(\frac{q(V - IR_s)}{nkT}\right)\left[1 - \exp\left(\frac{-q(V - IR_s)}{kT}\right)\right], \quad (1)$$

where V is the applied bias voltage, IR_s is voltage drop across series resistance of the diode, q is the electronic charge, n is the ideality factor, k is the Boltzmann constant, T is the temperature in K and I_o

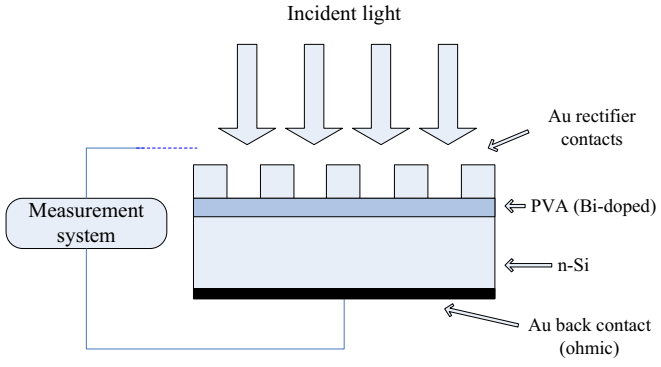

Fig. 1. Schematic cross-section of the device and measurement system.

is the reverse bias saturation current and can be extracted from the straight-line intercept of ln I–V plot at zero-bias and is given by:

$$I_o = AA^*T^2\exp\left(-\frac{q\Phi_{Bo}}{kT}\right), \tag{2}$$

where A is the rectifier contact area, A^* is the Richardson constant (120 A/cm^2 K^2 for n-type Si) and Φ_{Bo} is the zero bias apparent barrier height. The ideality factor is introduced to take the deviation of the experimental I–V data from the ideal thermionic emission (TE) theory into account and it can be obtained from the slope of straight-line of the forward bias ln I–V plot and can be written as:

$$n = \frac{q}{kT}\frac{d(V - IR_s)}{d(\ln(I))}, \tag{3}$$

The forward and reverse bias semi-logarithmic of the ln I–V characteristics of the Au/PVA (Bi-doped)/n-Si photodiode in dark and illumination conditions at room temperature is given in Fig. 2(a). As can be seen in Fig. 2(a), the forward bias the ln I–V characteristics in dark clearly indicates two distinct linear regions with different slopes in low bias ($0.08 < V < 0.42$) and in intermediate bias regions ($0.42 < V < 1.08$). In the high forward bias region ($V \geq 1.1$ V) the ln I–V plots deviated from the linearity due to the effect of R_s. On the other hand under illumination condition the first region starts to disappear due to its photovoltaic characteristics. As can be seen in Fig. 2(a) the open circuit voltage V_{oc} is about 0.42 V. Therefore only the first two regions in the I–V characteristics have importance for solar cell or photodiode applications since the V_{oc} for a Si based solar cell is usually less than 0.6 V and for a Si based photodiode is usually less than 0.4 V. Furthermore, it was shown in Fig. 2(a) that the recombination generation current component had no significant effect on the conversion efficiency in solar cells and photodiodes.

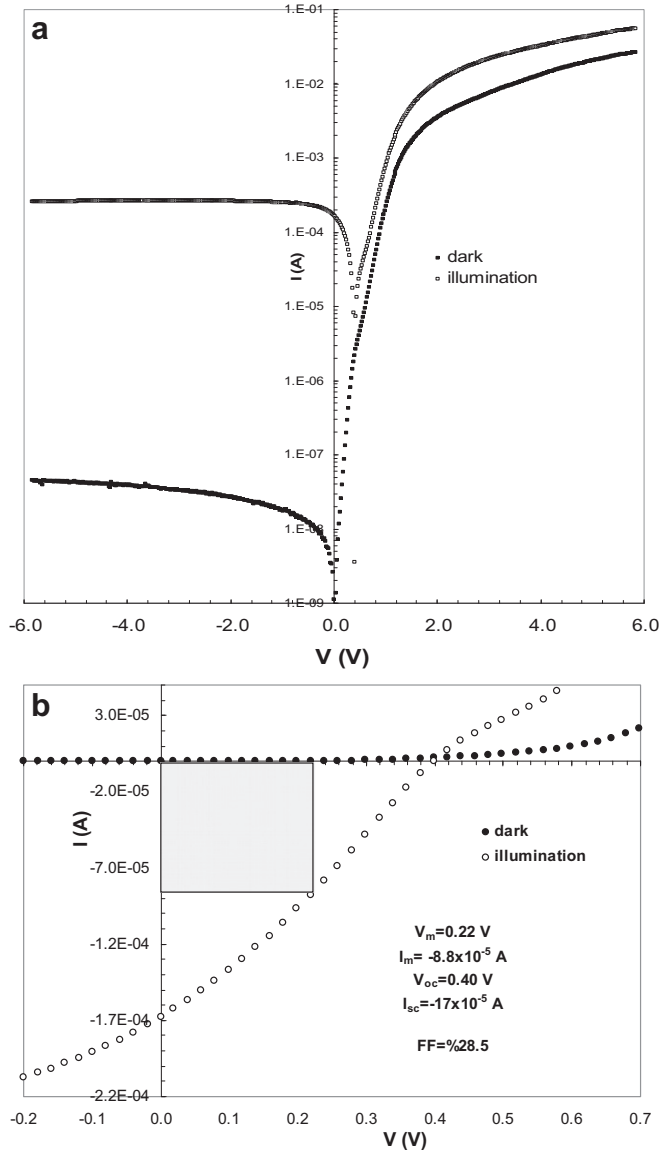

Fig. 2. (a) ln I–V, (b) I–V characteristics of Au/PVA (Bi-doped)/n-Si photodiode in dark and under illumination conditions at room temperature.

The linear behavior of the ln I–V characteristics in the low and intermediate voltage region clearly shows a double exponential relationship between the current and applied voltage as in the p–n junction and in the minority carrier MIS type SBD and solar cells are reported in the literature [23–27]. According to refs. [25–27] these two linear behaviors in the forward bias ln I–V characteristics in dark show two distinct barrier heights (BHs) in the parallel. Thus, the dark current can be expressed as [40],

$$I = I_{o1}\left[\exp\left(\frac{q(V - IR_s)}{n_1kT}\right) - 1\right] + I_{o2}\left[\exp\left(\frac{q(V - IR_s)}{n_2kT}\right) - 1\right] + \frac{(V - IR_s)}{R_{sh}}, \tag{4}$$

where I_{o1} and I_{o2} are the reverse saturation currents, n_1 and n_2 are the diode ideality factors. The equivalent circuit for two parallel diodes model is given in Fig. 3 [28]. In addition the first and second terms in equation (4) may describe the diffusion and recombination generation current components, respectively. The obtained experimental values of I_o, n and Φ_{Bo} for the Au/PVA(Bi-doped)/n-Si diode in dark and under illumination were given in Table 1. As can be seen in Table 1, the diode ideality factor for the second diode or II region is much higher than first diode or I region. This indicates that the value of n strongly depends on applied bias voltage. These high values of n can be attributed to the high density of N_{ss} localized at M/S interface and the effect of barrier inhomogeneities [8–11]. Also, the image-force effect, recombination–generation, and tunneling may be possible mechanisms that could lead to an ideality factor value greater than unity [11,12].

In order to determine the dominant current conduction mechanism in the whole forward bias region for the Au/PVA (Bi-doped)/n-Si photodiode, I–V characteristics was also drawn as double logarithmic and were given in Fig. 4. As can be seen in Fig. 4, each ln (I) vs ln (V) plots have three distinct linear regions with different slopes (region I: $V < 0.61$ V; region II: 0.61 V $< V < 1.42$ V; region III: $V > 1.42$ V). As can be seen, these three linear regions have different slopes that obey $I \propto V^m$ change, that is the current is directly proportional to applied bias voltage [29,30]. Here m is the slope of

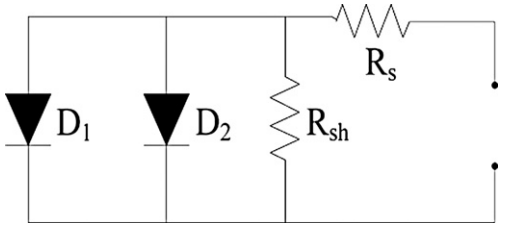

Fig. 3. The equivalent circuit for two parallel diodes model. D_1 and D_2 are the first and second diode, respectively, R_s is the series resistance and R_{sh} is the shunt resistance.

Table 1
Illumination dependence of various parameters determined from forward bias *I–V* characteristics of Au/PVA (Bi-doped)/n-Si photodiode.

	Region	I_o (A)	n	Φ_{Bo} (eV)	R_s ($dV/d\ln(I)$) (Ω)	R_s ($H(I)$) (Ω)
Dark	Low	1.86×10^{-9}	2.06	0.92	257.1	212.42
	High	9.95×10^{-8}	5.08	0.82		
Illumination (250 W)		7.58×10^{-8}	3.31	0.83	79.7	67.98

the ln (I) vs ln (V) plot for each linear regions and were found as 3.54, 5.96, 1.94 in dark and 3.69, 5.17, 1.58 under illumination, respectively. At low bias region (I), the current conduction mechanism exhibits an ohmic behavior. This behavior can be attributed to the superiority of bulk generated current in the film to the injected free carrier generated current. At the intermediate bias region current can be characterized by power law dependence. These behaviors obey the space-charge-limited-current (SCLC) theory that explains the increase in the injected electrons from the electrode to the films with the increasing applied bias voltage. The increase in the number of injected electrons causes filling up the traps and coming up the space charges [30,31]. At high bias region (III), because of the strong electron injection, the electrons escape from the traps and contribute to SCLC [30–33]. In this region, the current through the diode appears to become limited by another process and current values reveal that this limitation is not due to the R_s of the bulk Si or to the ohmic contact.

I–V characteristics and the photodiode parameters for the Au/Poly (vinyl alcohol) (Bi-doped)/n-Si photodiode at room temperature under 250 W illumination are shown in Fig. 2(b) by using Ohm law's the series resistance (R_s) and shunt resistance (R_{sh}) under illumination were estimated to be (Fig. 5) 96 Ω and 18.2 kΩ. This high series resistance of the photodiode accounted for the small fill factor (*FF*) and limited the conversion efficiency (τ). However in this study it was not aimed at optimizing the fabrication parameters to obtain the photodiode or solar cell with a high efficiency. The values of open-circuit voltage (V_{oc}), shortcircuit current (I_{sc}) and the fill factor (*FF*) for the Au/Poly (vinyl alcohol) (Bi-doped)/n-Si photodiode at room temperature under 250 W illumination level were found to be as 0.22 V, 8.853×10^{-5} A and 28.5%, respectively. This

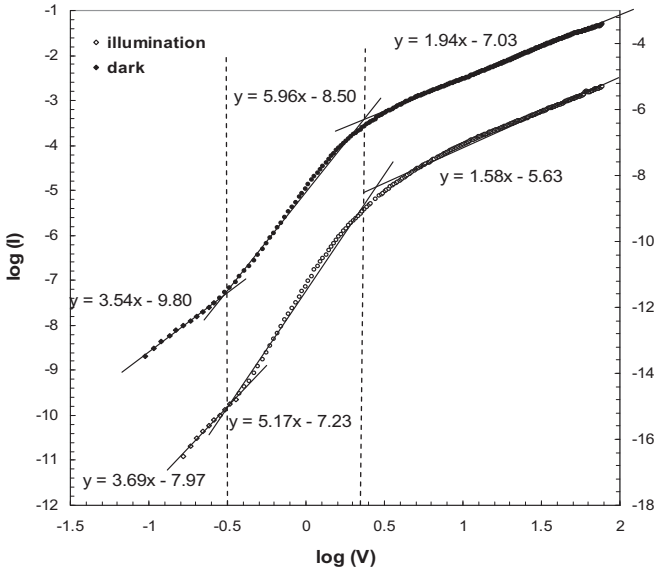

Fig. 4. The ln (I) vs ln (V) characteristics of the Au/PVA (Bi-doped)/n-Si photodiode in dark and under illumination conditions at room temperature.

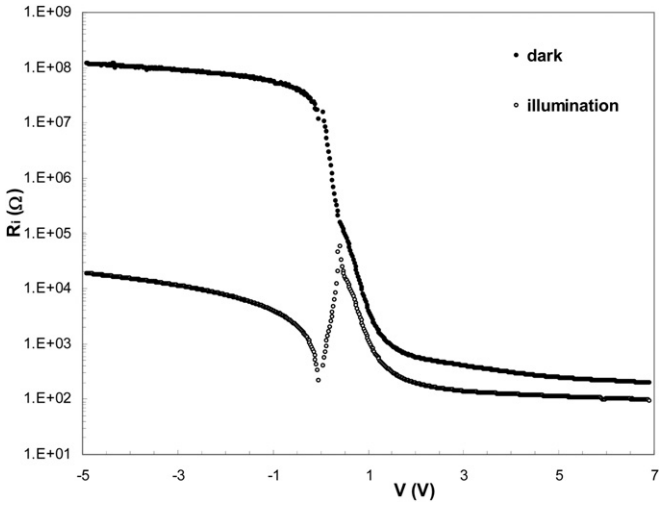

Fig. 5. The voltage dependent structure resistance of the Au/PVA (Bi-doped)/n-Si photodiode in dark and under illumination conditions at room temperature.

value of *FF* may be accepted sufficiently high for the Au/Poly (vinyl alcohol) (Bi-doped)/n-Si photodiode. Therefore, the fabricated SDs with a thin Bi-doped interfacial polymer layer are more sensitive to light, proposing them as a good candidate as a photodiode or optical sensor for optoelectronic applications.

The R_s and R_{sh} of photodiode are important parameters. These parameters influence the performance of the photodiode. Therefore, both the R_s and R_{sh} values were determined from the structure resistance (R_i) vs applied bias voltage (V_i) plots in dark and under illumination conditions, where $R_i = dV_i/dI_i$ and was given in Fig. 5. It was observed that at sufficiently high forward bias voltages the structure's resistance value approach to a constant value which is corresponding to R_s of the photodiode. The values of R_s were found as 200 Ω in dark and 96 Ω under illumination, respectively. Similarly, at sufficiently high reverse bias voltages the structure resistance values approach to a constant which is also corresponding to R_{sh} of the diode. Thus, the values of R_{sh} were found as 1.161×10^8 Ω in dark and 1.815×10^4 Ω under illumination, respectively.

When the value of R_s is sufficiently high, the linear range of the forward bias ln *I–V* curves may be reduced. In this case, the accuracy of the determination of Φ_{Bo} and n becomes poorer and unreliable. Therefore, the R_s, n and Φ_{Bo} values were also achieved using a method developed by Cheung and Cheung [34] in the downward curvature (non-linear region) of the forward bias *I–V* characteristics. According to this method from Eq. (1), following functions can be written as:

$$\frac{dV}{d\ln(I)} = IR_s + \left(\frac{nkT}{q}\right), \tag{5}$$

$$H(I) = V - \left(\frac{nkT}{q}\right) Ln\left(\frac{I}{AA^*T^2}\right) = IR_s + n\Phi_B, \tag{6}$$

In Fig. 6(a) and (b), experimental $dV/d(\ln I)$ vs I and $H(I)$ vs I plots are presented for Au/PVA (Bi-doped)/n-Si photodiode in dark and under illumination, at room temperature. As can be seen in these figures, Eqs. (5) and (6) give a straight line for the data of downward curvature region (region III) in the forward bias ln *I–V* characteristics. Where Φ_B is the barrier height obtained from data of downward curvature region in the forward bias ln *I–V* characteristics. Thus, the n and R_s were determined from the intercept and slope of $dV/d(\ln I)$ vs I plots (Fig. 6(a)) in dark and under illumination conditions at room temperature. After then using the n value determined from Eq. (5) and the data of downward curvature

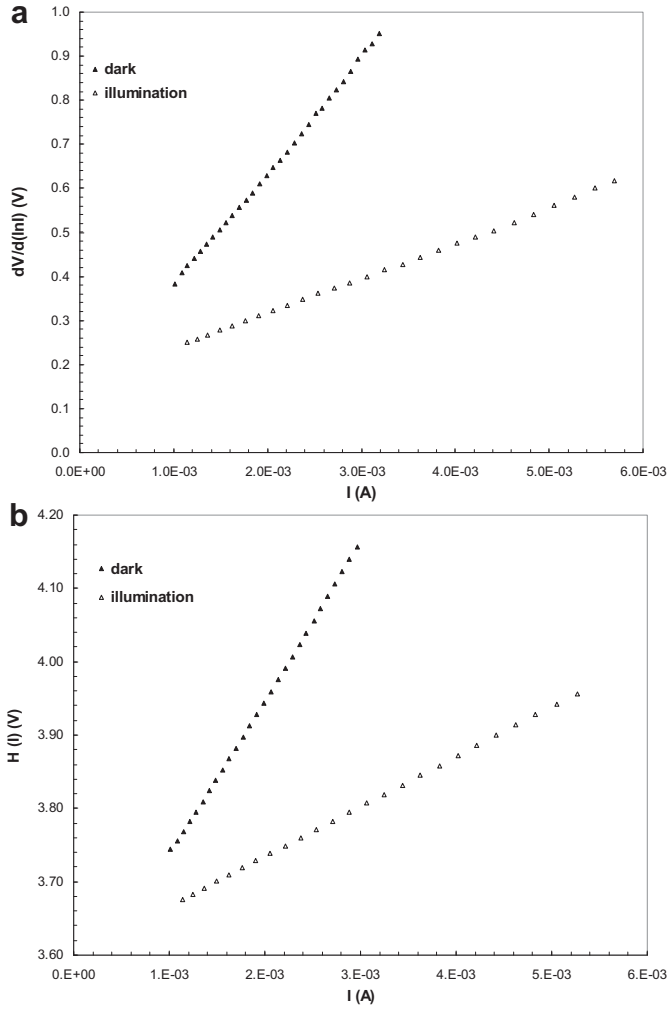

Fig. 6. (a) Experimental dV/dln I vs I and (b) $H(I)$ vs I plots of Au/PVA (Bi-doped)/n-Si photodiode in dark and under illumination conditions at room temperature.

region in the forward bias I–V characteristics in Eq. (6) a plot of $H(I)$ vs I plots (Fig. 6(b)) will also lead a straight line with y-axis intercept equal to $n\Phi_B$. The slope of this plot also provides a second determination of Rs, which can be used to check the consistency of this approach. As function of illumination, the values of four main diode parameters (n, Φ_B, I_0 and Rs) were obtained and also presented in Table 1. As shown in Table 1, these values obtained by different methods are almost in agreement with each other and decrease with illumination. Similar results have been reported in the literature [35–37]. The results are consistent with a net reduction in carrier density in the depletion region of device through the introduction of traps and recombination centers associated with illumination effect [38].

The energy density distribution of the interface states (N_{ss}) in equilibrium with the semiconductor can be determined from the forward bias I–V data by taking the voltage dependent ideality factor n(V) and effective barrier height (Φ_e)into account. The quantities of n(V) and (Φ_e) can be described as following equations, respectively [9].

$$n\left(V\right) = \frac{q}{kT}\left[\frac{(V - IR_s)}{\ln(I/I_o)}\right] = 1 + \frac{\delta}{\varepsilon_i}\left[\frac{\varepsilon_s}{W_D} + qN_{ss}\left(V\right)\right], \tag{7}$$

$$\Phi_e = \Phi_{Bo} + \beta(V - IR_S) = \Phi_{Bo} + \left(1 - \frac{1}{n(V)}\right)(V - IR_S), \tag{8}$$

where β (=dΦ_e/dV = 1 − 1/$n(V)$) is the voltage coefficient of the effective barrier height Φ_e used in place of the barrier height Φ_{Bo} and it is a parameter that includes the effects of both interface states in equilibrium with the semiconductor. Density of interface states proposed by Card and Rhoderick can be simplified and given as [9]:

$$N_{ss}\left(V\right) = \frac{1}{q}\left[\frac{\varepsilon_i}{\delta}(n(V) - 1) - \frac{\varepsilon_s}{W_D}\right], \tag{9}$$

where δ is the thickness of interfacial insulator layer, W_D is the depletion layer width, $\varepsilon_i = 3.8\ \varepsilon_0$, $\varepsilon_s = 11.8\ \varepsilon_0$ are permittivity of the interfacial insulator layer and the semiconductor, respectively, and ε_0 is the permittivity of the free space charge. Furthermore in n-type semiconductors, the energy of interface states N_{ss} with respect to the bottom of conduction band E_c at the surface of the semiconductor can be obtained according to refs. [9,11]. The value of W_D is obtained from the experimental C^{-2}–V plot for each illumination level at 1 MHz. Furthermore, for n-type semiconductors, the energy of the interface states E_{ss} with respect to the bottom of the conduction band at the surface of semiconductor is given as:

$$E_c - E_{ss} = q(\Phi_e - V), \tag{10}$$

substituting in Eq. (8) the values of the voltage dependence of n (V), δ and W_D, the values of N_{ss} as a function of ($E_c - E_{ss}$) were obtained and are given in Fig. 7. As shown in Fig. 7, the exponential growth of the N_{ss} from midgap toward the bottom of conduction band is very apparent. In addition, the values of N_{ss} increase with increasing illumination between the (E_c − 0.43) and (E_c − 0.71) eV.

3.2. Effects of illumination on the C–V and G/ω–V characteristics

Both in the dark and under illumination, C–V and G/ω–V characteristics of Au/PVA (Bi-doped)/n-Si photodiode in both reverse and forward bias voltages were measurement at room temperature and 1 MHz frequency and were given in Fig. 8 (a) and (b), respectively. As can be seen in Fig. 8, both the values of C and G/ω increase under illumination condition especially in depletion and inverse regions. When photons' energy is greater than energy band gap of semiconductor (E_g), it may lead to generation of electron hole pairs

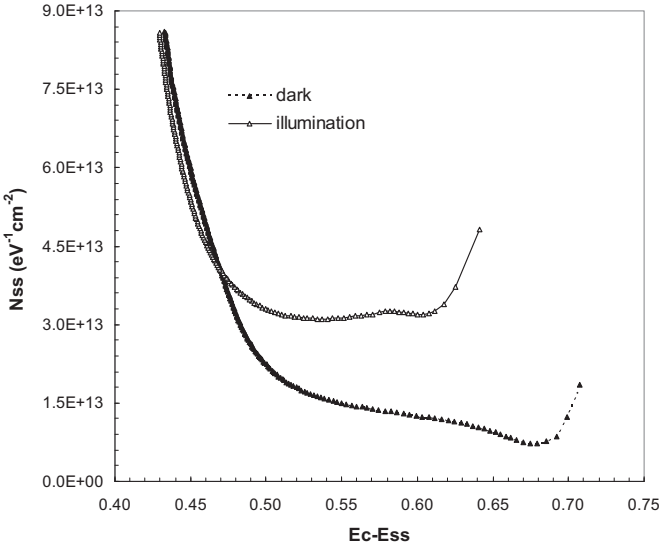

Fig. 7. The energy distributions profile of the N_{ss} with obtained from the forward bias I–V characteristics of Au/PVA (Bi-doped)/n-Si photodiode in dark and under illumination conditions at room temperature.

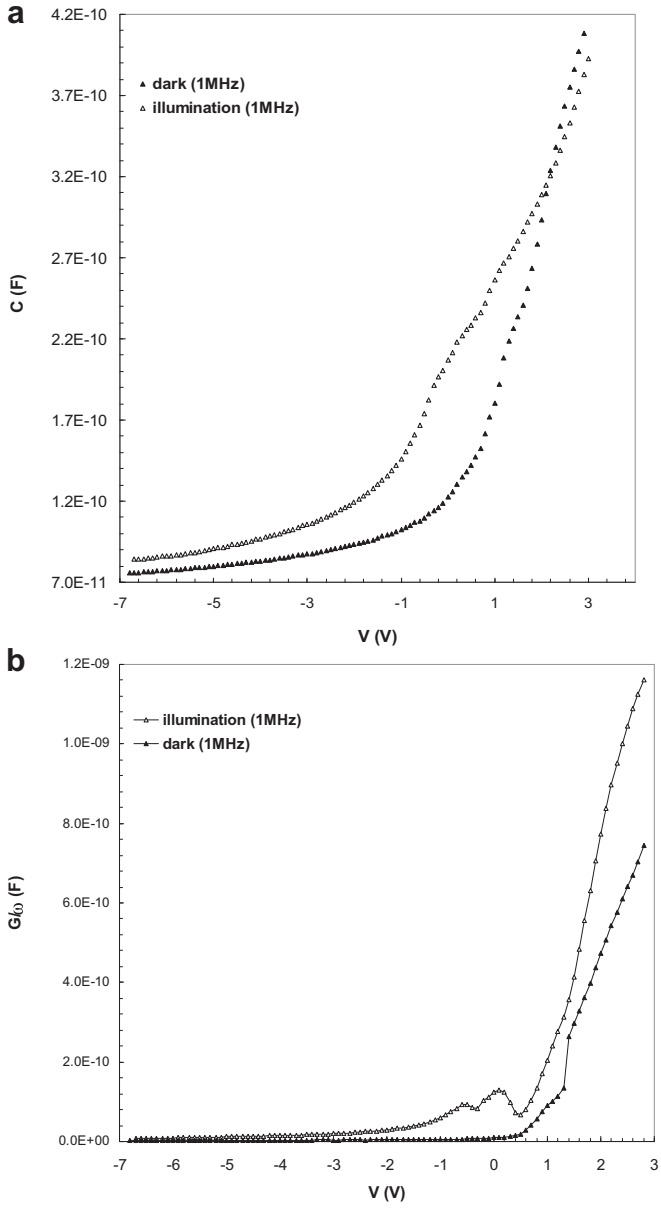

Fig. 8. (a) Measured forward and reverse bias capacitance (b) conductance curves of Au/PVA (Bi-doped)/n-Si photodiode in dark and under illumination conditions at room temperature.

in the depletion region of the semiconductor. After that, the structures are stressed with an electric field, these electron–hole pairs would be separated by the strong local internal electric field at grain boundaries. Electrons are swept out of the insulator/polymer layer quickly by the electric field while the holes are swept slowly and hence could be trapped by the defects. Consequently, there would be an additional photo capacitance and conductance in the diode.

The voltage dependent of interface states profile was found by using the dark and illumination capacitance data as following [39],

$$N_{ss}\left(V\right) = \frac{1}{qA}\left[\left(\frac{1}{C_{dark}}-\frac{1}{C_{ox}}\right)^{-1}-\left(\frac{1}{C_{ill}}-\frac{1}{C_{ox}}\right)^{-1}\right], \tag{11}$$

where C_{dark} and C_{ill} are the measurement capacitance in dark and under illumination conditions, respectively, A is the area of rectifier contact and q is the electronic charge. The advantage of this method

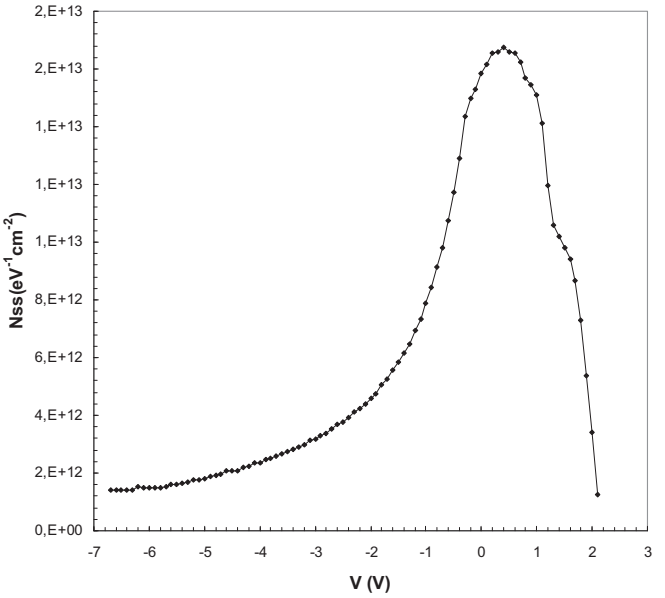

Fig. 9. The energy distribution profile of the N_{ss} obtained from dark-illumination capacitance technique of Au/PVA (Bi-doped)/n-Si photodiode.

comes from the fact that it permits determination of many properties of the insulating interface layer, the semiconductor substrate, and interface easily. In this method [39], the N_{ss} is extracted from its capacitance contribution to the measured experimental C–V curve. In the equivalent circuit of MIS and MPS type SBDs, the oxide/insulator capacitance C_{ox} is in series with the parallel combination of the interface trap or surface states capacitance (C_{it}) and the space charge capacitance (C_{sc}). In general, in dark and at high frequency, N_{ss} cannot respond to the ac excitation, so they do not contribute to the total capacitance and conductance directly. The density distribution of interface states profile as function of applied bias voltage is given in Fig. 9. As shown in Fig. 9, the N_{ss}–V plot gives a peak at about 0.45 V. The values of N_{ss} are of the order about 10^{13} eV cm^{-2}, which is high enough to pin Fermi level of the Si substrate surface [40].

4. Conclusion

The forward and reverse bias I–V, C–V and G/ω–V characteristics of the fabricated Au/PVA (Bi-doped)/n-Si photodiode have been investigated in dark and under 250 W illumination intensity at room temperature. The main electrical parameters such as n, Φ_{B0}, N_{ss}, R_{sh} and R_s of the photodiode were found as strong functions of illumination. The high value of n and R_s have been attributed to the particular distribution of N_{ss} at metal/PVA interface, surface and fabrication processes, barrier inhomogeneity of interfacial polymer layer and barrier height at M/S interface. These changes in the main electrical parameters can be attributed that electron–hole pairs generate in the junction as a result of the photons absorption. The values of C and G/ω were also as found strong functions of illumination. The energy density distribution profile of N_{ss} was extracted from the forward bias I–V measurements by taking into the voltage dependence of Φ_e and R_s for photodiode in dark and under 250 W illumination intensity account. In addition the voltage dependent N_{ss} profile was obtained from the dark and illumination capacitance at 1 MHz. The obtained values of N_{ss} from these two methods are in agreement with each other and about 10^{13} eV cm^{-2}. The values of R_s and R_{sh} of photodiode were determined from the R_i–V_i plots as 200 Ω and 1.161×10^8 Ω (in dark) and 96 Ω and 1.815×10^4 Ω (under 250 W), respectively. Experimental results show that the fabricated

structure can be used as a photodiode or photo-capacitance sensor in modern electronic industry.

References

[1] M. Soylu, F. Yakuphanoğlu, Thin Solid Films 519 (2011) 1950.
[2] G.B. Sakr, I.S. Yahia, J. Alloys Compd. 503 (2010) 213.
[3] B. Akkal, Z. Benemara, N. Bachir Bouiadjra, S. Tizi, B. Gruzza, Appl. Surf. Sci. 253 (2006) 1065.
[4] H. Uslu, Ş. Altındal, U. Aydemir, İ. Dökme, İ.M. Afandiyeva, J. Alloys Compd. 503 (2010) 96.
[5] F. Yakuphanoğlu, Y.S. Ocak, T. Kılıçoğlu, W.A. Farooq, Microelectron. Eng. 88 (2011) 2951.
[6] A.A.M. Farag, J. Alloys Compd. 509 (2011) 8056.
[7] Y.S. Ocak, M. Kulakcı, R. Turan, T. Kılıçoğlu, O. Gullu, J. Alloys Compd. 509 (2011) 6631.
[8] T. Tunç, Ş. Altındal, İ. Dökme, H. Uslu, J. Electron. Mater. 40 (2) (2011) 157.
[9] H.C. Card, E.H. Rhoderick, J. Phys. D Appl. Phys. 4 (1971) 1589.
[10] S. Demirezen, Z. Sönmez, U. Aydemir, Ş. Altındal, Curr. Appl. Phys. 12 (2012) 266.
[11] R.T. Tung, Phys. Rev. B 45 (23) (1992) 13509.
[12] Ö. Güllü, Int. J. Photoenergy 2009 (2009) 374301.
[13] D. Bjorge, N. Daels, S.D. Vrieze, P. Dejans, T.V. Camp, W. Audenaert, J. Hogie, P. Westbroek, K.D. Clerck, S.W.H.V. Hulle, Desalination 249 (2009) 942.
[14] Y. Yokoyama, S. Hattori, C. Yoshikawa, Y. Yasuda, H. Koyama, T. Takato, H. Kobayashi, Mater. Lett. 63 (2009) 754.
[15] B.P. Timko, T. Cohen-Karni, G.H. Yu, Q. Qing, B.Z. Tian, C.M. Lieber, Nano Lett. 9 (2009) 914.
[16] T.J. Kempa, B. Tian, D.R. Kim, J. Hu, X. Zheng, C.M. Lieber, Nano Lett. 8 (2008) 3456.
[17] P. Viswanathamurthi, N. Bhattarai, H.Y. Kim, D.R. Lee, Nanotechnology 15 (2004) 320.
[18] G.N.S. Vijayakumar, S. Devashankarb, M. Rathnakumarib, P. Sureshkumar, J. Alloys Compd. 507 (2010) 225.
[19] W.P. Kang, J.L. Davidson, Y. Gurbuz, D.V. Kerns, J. Appl. Phys. 78 (1995) 1101.
[20] M. Gökçen, T. Tunç, Ş. Altındal, İ. Uslu, Mater. Sci. Eng. B Adv. Funct. Solid-state Mater. 177 (5) (2012) 416.
[21] R.F. Bhajantri, V. Ravindrachary, A. Harisha, C. Ranganathaiah, G.N. Kumaraswamy, Appl. Phys. A Mater. Sci. Process. 87 (2007) 797.
[22] R.K. Gupta, K. Ghosh, P.K. Kahol, Curr. Appl. Phys. 9 (2009) 933.
[23] M.A. Green, F.D. King, J. Shwechun, Solid-State Electron. 17 (1974) 551.
[24] J. Shewchun, M.A. Green, F.D. King, Solid-State Electron. 17 (1974) 563.
[25] D. Defives, O. Noblanc, C. Dua, C. Brylinski, M. Barthula, b. Aubry-Fortuna, F. Meyer, IEEE Trans. Electron. Dev. 46 (1999) 449.
[26] D.J. Ewing, L.M. Portter, Q. Wahab, X. Ma, T. Sudarshan, S. Tumakha, M. Gao, L.J. Brillson, J. Appl. Phys. 101 (2007) 114514.
[27] B.J. Skromme, E. Luckowski, K. Moore, M. Bharnagar, C.E. Weitzel, T. Gehoski, D. Ganser, J. Electron. Mater. 29 (2000) 376.
[28] M. Saad, A. Kassis, Sol. Energy Mater. Sol. C 77 (2003) 415.
[29] S. Kar, W.E. Dahlke, Solid-State Electron. 15 (1972) 221.
[30] S. Wagle, V. Shirodkar, Braz. J. Phys. 30 (2) (2000) 380.
[31] Y.S. Ocak, M. Kulakci, T. Kılıcoglu, R. Turan, K. Akkılıc, Synth. Met. 159 (2009) 1603.
[32] H. Wang, X.N. Shen, X.J. Su, Z. Wang, S.X. Shang, M. Wang, Ferroelectrics 195 (1997) 233.
[33] O. Gullu, S. Aydogan, A. Turut, Microelectron. Eng. 85 (2008) 1647.
[34] S.K. Cheung, N.W. Cheung, Appl. Phys. Lett. 49 (1986) 85.
[35] A.A.M. Farag, I.S. Yahia, M. Fadel, Int. J. Hydrogen Energy 34 (2009) 4906.
[36] F. Yakuphanoğlu, Sensor Actuat. A Phys. 147 (2008) 104.
[37] K. Akkılıç, F. Yakuphanoğlu, Microelectron. Eng. 85 (2008) 1826.
[38] M.Y. Feteha, M. Soliman, N.G. Gomaa, M. Ashry, Renew. Energy 26 (2002) 113.
[39] E.H. Nicollian, J.R. Brews, MOS Physics and Technology, Wiley, New York, 1982.
[40] N. Konofaos, Microelectron. J. 35 (2004) 421.